

**Anomalous relaxation in a quasi-one-dimensional fractal cluster glass**S. J. Etzkorn,<sup>1</sup> Wendy Hibbs,<sup>2</sup> Joel S. Miller,<sup>2</sup> and A. J. Epstein<sup>1,3</sup><sup>1</sup>*Department of Physics, The Ohio State University, Columbus, Ohio 43210-1106, USA*<sup>2</sup>*Department of Chemistry, University of Utah, Salt Lake City, Utah 84112-0850, USA*<sup>3</sup>*Department of Chemistry, The Ohio State University, Columbus, Ohio 43210-1173, USA*

(Received 19 April 2004; published 27 October 2004)

The low-temperature spin glass state of the quasi-1D organic-based magnet  $[\text{MnTPP}]^+[\text{TCNE}]^- \cdot x(1,3\text{-C}_6\text{H}_4\text{Cl}_2)$  has unusually long relaxation times due to frustration induced by dipole-dipole interactions between fractal spin clusters. This long relaxation is investigated with in-field relaxation measurements. The extremely long relaxation process enables probing of time-dependent phenomena using conventional magnetic measurements, including sweep rate-dependent hysteresis curves, even for temperatures well above the spin glass transition temperature ( $T_g$ ). For a temperature of  $\sim 1.3T_g$ , the coercive field increased by 170% for differing sweep rates, while below  $T_g$  the change was less than 5%. A study of the temperature dependence of the coercive field reveals detailed information on the behavior of fractal spin clusters within the system. For temperatures above  $T_g$ , the largely single-chain spin clusters act independently during magnetic reversal. As the spin clusters branch out below  $T_g$ , magnetic reversal is more cooperative, reflecting an enhancement of the magnetic interaction in the interpenetrating fractal cluster system.

DOI: 10.1103/PhysRevB.70.134419

PACS number(s): 75.50.Lk, 75.10.Nr, 75.60.Ej, 75.60.Jk

**I. INTRODUCTION**

Dipole-dipole interactions are nearly always ignored when analyzing magnetic systems. Typically, these interactions are insignificant when compared with the larger direct exchange interaction. However, these interactions are important in several systems, including organic-based magnets,<sup>1-3</sup> pyrochlore spin ice materials,<sup>4,5</sup> and frozen ferrofluids.<sup>6-8</sup> Among these, the manganeseporphyrin family of organic-based magnets provides a unique platform to study the impact of dipole-dipole interactions in a highly anisotropic system.

The manganeseporphyrin family of magnets forms one-dimensional (1D) polymers with large, chemically tunable ( $\sim 10$  to over  $20 \text{ \AA}$ ) interchain spacing.<sup>9</sup> High-temperature magnetic data agree<sup>1,9-11</sup> with a model of alternating quantum and classical spins.<sup>12</sup> Bulk magnetic order at lower temperatures results from dipolar interactions among chains, as the large interchain spacing eliminates viable exchange pathways.<sup>1,10,11</sup> Competition between interchain dipole-dipole interactions and the single-ion anisotropy of the metal ion leads to frustration and spin glass ordering at low temperatures.<sup>1,13</sup>

The spin glass transition occurs near 4 K for the manganeseporphyrin magnet  $[\text{MnTPP}]^+[\text{TCNE}]^- \cdot x(1,3\text{-C}_6\text{H}_4\text{Cl}_2)$  (TPP is tetraphenylporphyrin dianion, TCNE is tetracyanoethylene). Recent studies<sup>13</sup> report the transition to the frozen state occurs as correlated spin clusters within the material grow in both size and fractal dimension. The results from this previous study show that near the spin glass transition, the spin clusters are centered on single chains with correlations branching into other chains. The transition is viscous, covering a large range in both temperature and relaxation times, which provides a unique platform for the study of magnetic relaxation.

We report here the results of a study of the magnetic relaxation of  $[\text{MnTPP}]^+[\text{TCNE}]^- \cdot x(1,3\text{-C}_6\text{H}_4\text{Cl}_2)$  which

probes the role of the fractal nature of the spin clusters in relaxation and magnetic reversal. In-field relaxation measurements reveal stretched exponential behavior similar to magnetic decay data previously reported.<sup>13</sup> This relaxation occurs on very long time scales due to the fractal nature of the system, and has marked impact on typical magnetic measurements. Dynamic hysteresis measurements were taken both above and below the glass transition, providing insight to magnetic reversal as the fractal spin clusters evolve. Hysteresis measurements well above the glass transition temperature ( $T_g$ ) exhibit an effective coercive field ( $H_c$ ) which is strongly dependent on the sweep rate of the applied magnetic field. The temperature dependence of  $H_c$  below  $T_g$  is linear revealing a temperature-independent energy barrier responsible for coercivity in the frozen state. This collective behavior demonstrates the impact of the branching of spin clusters into neighboring chains within an anisotropic fractal cluster model. The interlocked fractal spin clusters increase the strength of the interaction between clusters which enhances the effective coercivity of the system. A crossover in the temperature dependence of  $H_c$  from linear to more complex behavior occurs at 5 K just above  $T_g$ . This crossover occurs as the spin clusters are reduced to being located on single chains and begin to act independently rather than cooperatively. The system near  $T_g$  was shown to behave as a collection of fractal spin clusters; attempts to model the relaxation with simple 1D models were unsuccessful.

**II. EXPERIMENTAL**

Polycrystalline samples of  $[\text{MnTPP}]^+[\text{TCNE}]^- \cdot x(1,3\text{-C}_6\text{H}_4\text{Cl}_2)$  were synthesized according to Ref. 9. In order to avoid rotation of the highly anisotropic<sup>14</sup> polycrystalline powder, samples were constrained for study by dispersing it in eicosane (melting point  $36\text{--}38^\circ\text{C}$ ), heating above  $40^\circ\text{C}$  and subsequently cooling to room temperature. The prepared

samples were then sealed in quartz tubes or airtight Delrin® sample holders. Measurements for dc magnetization were taken on either a Quantum Design MPMS-5 SQUID magnetometer or a Quantum Design PPMS-9 with the ACMS option. Results from both instruments are in excellent agreement. The ac susceptibility was measured with a LakeShore 7225 ac susceptometer/dc magnetometer. The instrument was calibrated for both phase and relative amplitude at each frequency by the use of a paramagnetic standard.

Magnetization measurements were recorded for various applied fields, over a temperature range from 2.0 to 50 K. The sample was cooled to the lowest measured temperature either in the desired applied field (FC) or in zero applied field (ZFC) with the desired field subsequently applied. Magnetization was then recorded upon warming the sample. In order to observe dynamic effects, the magnetization was recorded after waiting different periods of time prior to measurement after the temperature had stabilized.

Magnetic hysteresis measurements were made for temperatures from 2.0 to 6.0 K with uniform steps in magnetic field. In order to observe time-dependent characteristics, hysteresis loops were recorded for different sweep rates of the magnetic field. For each sweep rate, the magnetic field was ramped linearly, with measurements taken upon reaching the desired value of the applied magnetic field. In addition measurements were taken with the magnet in a *static mode*, for which the superconducting magnet was placed in the persistent state (removed from the current source) at the desired applied field before measurement of the magnetization. For both types of hysteresis loops, care was taken to reduce the remanent field from the superconducting magnet to  $< 1$  Oe.

### III. EXPERIMENTAL RESULTS

#### A. FC/ZFC magnetization

Magnetization data were collected for fields ranging from 5.0 to 1000 Oe. The data were recorded upon warming after waiting a period of  $\sim 5$  s after the temperature had stabilized. The data show spin-glass-like behavior, with a strong irreversibility between the FC and ZFC states of the system. Below  $\sim 5$  K both the FC and ZFC magnetization remains at a constant value consistent with a frozen spin glass state. The value of the ZFC magnetization is approximately the same for all recorded values of the applied field below  $\sim 5$  K.

In order to observe dynamic effects, FC/ZFC data for a 10 Oe applied field were recorded for various waiting times at the desired temperature prior to measurement. The results (Fig. 1) show a small, but distinct shift in the bifurcation point for data of different waiting times. The bifurcation point shifts to lower temperatures with longer waiting times. However, even for the longest waiting time measured (30 min), this bifurcation point occurs at  $\sim 5$  K, well above the glass transition of 4.1 K as determined from a scaling analysis of the ac susceptibility.<sup>13</sup>

#### B. Hysteresis measurements

Time-dependent effects in the isothermal hysteresis loops were observed by taking data for three different sweep rates

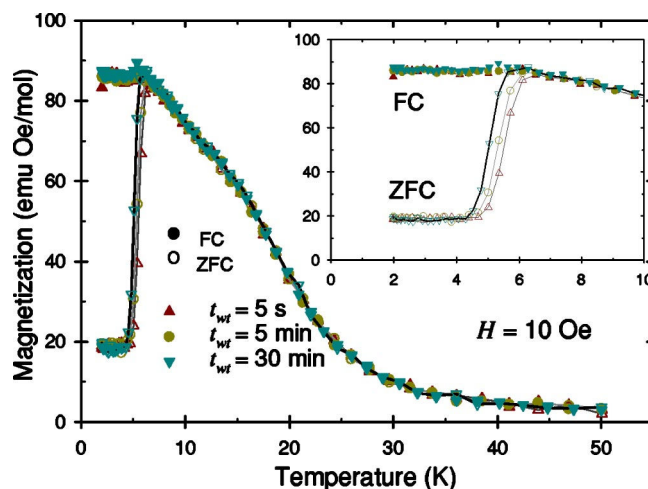


FIG. 1. (Color online) FC and ZFC magnetization curves for  $[\text{MnTPP}]^+[\text{TCNE}]^- \cdot x(1,3\text{-C}_6\text{H}_4\text{Cl}_2)$  recorded at 10 Oe applied field for various waiting times at each temperature prior to measurement. The inset plots the same data over a smaller temperature region showing the small but reproducible shift due to time dynamics.

of the applied magnetic field (10.7, 53.5 and 107.0 Oe/s). The magnetization was recorded at equal intervals in field up to 50 kOe with 100 Oe steps at 5.2 K and 1250 Oe steps at 2.5 K. The extraction technique utilized by the magnetometer (PPMS) operated at a speed of 100 cm/s which significantly reduces any errors due to the sweeping of the magnetic field.

Even well above  $T_g$  (4.1 K), a clear change in the hysteresis of the sample for the different sweep rates of the magnetic field is evident [Fig. 2(a)]. At 5.2 K ( $\sim 1.3T_g$ ) the field required for reversal of the magnetization, the effective coercive field  $H_c$  changes by 170% between the 10.7 and 107 Oe/s sweep rates. However, for temperatures well below  $T_g$ , the hysteresis loops for the different rates are nearly identical [ $< 5\%$  change, see Fig. 2(b)]. The value for  $H_c$  at 2.5 K is quite large ( $\sim 20$  kOe) consistent with the large values observed in other manganeseporphyrin linear chain magnetic materials.<sup>15,16</sup>

Hysteresis loops also were recorded without applying a field large enough to achieve saturation. These minor loops were studied with the initial magnetization curve both in the direction of positive (forward) and negative (reverse) applied field at a temperature of 5.0 K with a field range of  $-300$  to  $+300$  Oe. The resultant loops (Fig. 3) are strongly shifted from each other, with the forward loop shifted up and the reverse loop shifted down from the origin. The loops possess a very rounded shape at the edges and remain open upon completing the cycle. Data also were taken at 2.5 K, however these loops below  $T_g$  were closed and showed no shift between the forward and reverse directions.

Full saturation hysteresis loops taken in the static mode between 2.0 and 6.0 K enabled an investigation of  $H_c(T)$ . Due to the dynamic nature of the hysteresis above  $T_g$  [Fig. 2(a)], care was taken to insure that data above  $T_g$  were taken under the exact same time altering conditions, such as field step size and density of data points. These steps were taken

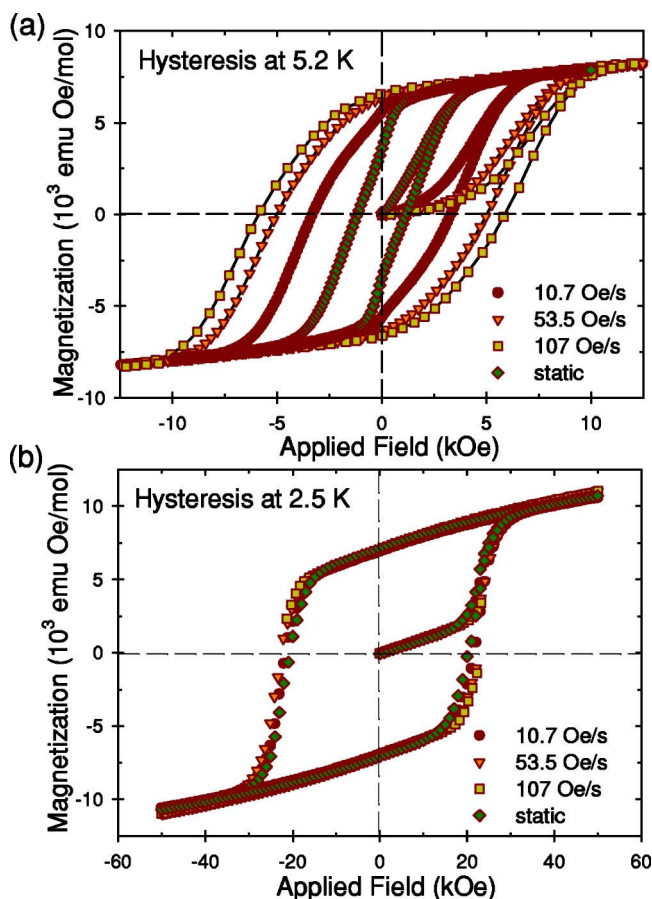


FIG. 2. (Color online) Hysteresis curves of  $[\text{MnTPP}]^+[\text{TCNE}]^-\cdot x(1,3\text{-C}_6\text{H}_4\text{Cl}_2)$  for different sweep rates of the applied magnetic field. (a) Above  $T_g$ , the hysteresis curve, and  $H_c$ , is strongly dependent on the sweep rate. (b) Below  $T_g$ , the curves are nearly identical.

to provide a consistent set of measurements to analyze the temperature dependence. It should be noted that the conditions used for these temperature dependent measurements were not the same as those used for the dynamic data of Fig. 2.<sup>20</sup> The results (Fig. 4) show a linear dependence of  $H_c$  on  $T$  up to temperatures of 5.0 K as reported for a related system.<sup>15</sup> Above 5.0 K, the temperature dependence of  $H_c$  is more complex and as suggested by Fig. 2(a) is strongly dependent on the time scale of measurement. For measurements performed in the static mode described above, the data for temperatures above 5.3 K can be fit with a function of the form<sup>17</sup>

$$\left(\frac{H_c}{H_0}\right)^{3/7} = 1 - aT^{2/3}, \quad (1)$$

where  $H_0$  and  $a$  are fitting constants.

### C. In-field relaxation

The dynamic response of the system to a magnetic field was probed at various points on the initial magnetization curve. Data were recorded as magnetization versus time for temperatures above and below the expected glass transition

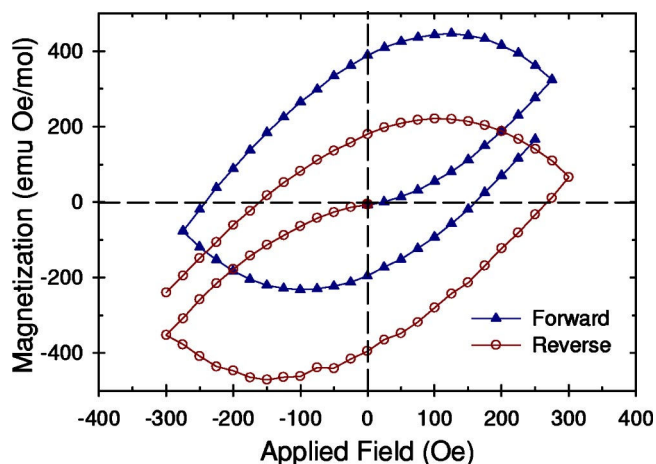


FIG. 3. (Color online) Comparison of minor hysteresis loops of  $[\text{MnTPP}]^+[\text{TCNE}]^-\cdot x(1,3\text{-C}_6\text{H}_4\text{Cl}_2)$  at 5.0 K in both the forward (+ $H$ ) and reverse ( $-H$ ) directions. The curves show the magnetic history-dependent nature of the hysteresis loops as a result of magnetic relaxation.

temperature. The magnetic field values were chosen to place the system either on the first flat portion of the S-shaped initial magnetization curve or on the more vertical section. For a temperature of 5.0 K, these  $H$  values correspond to 100 and 1000 Oe, respectively, while for  $T=2.5$  K the chosen fields were 17.5 and 2.25 kOe. The results of the magnetic relaxation in this manner are shown in Fig. 5. The best achievable fit to the expected stretched exponential<sup>13</sup>

$$M(t) = M_0 + \sigma_0(1 - e^{-(t/\tau)^{1-n}}) \quad (2)$$

is also shown.

A large discrepancy is observed in the saturation value of the magnetization for the fields at 5.0 K [Fig. 5(a)]. The fits to the data at 5.0 K are quite good and both yield a value for  $\tau$  near 5000 s ( $\tau=5627$  and 5181 s for 100 and 1000 Oe,

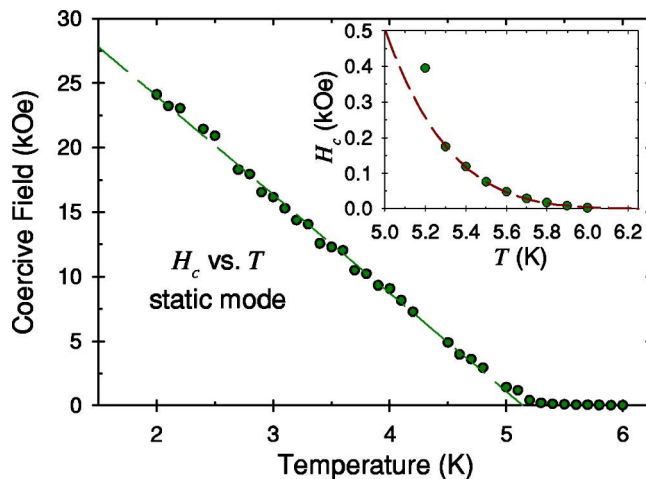


FIG. 4. (Color online)  $H_c(T)$  for  $[\text{MnTPP}]^+[\text{TCNE}]^-\cdot x(1,3\text{-C}_6\text{H}_4\text{Cl}_2)$  in the static mode, the inset shows a close-up for temperatures above 5.0 K. The dash lines in the figure and the inset correspond to fits to a straight line and Eq. (1), respectively.



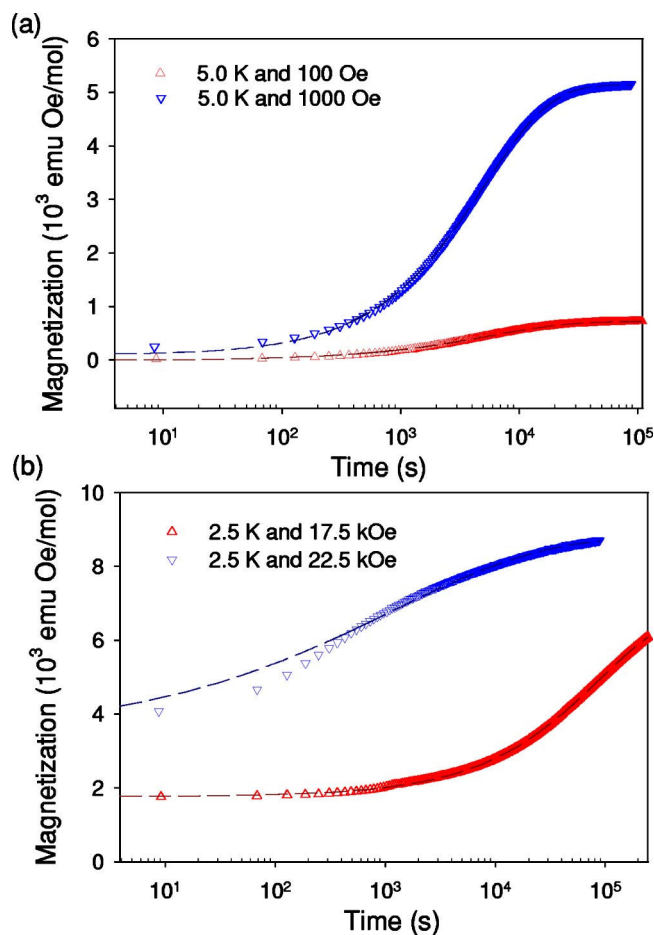


FIG. 5. (Color online) Magnetic relaxation in  $[\text{MnTPP}]^+[\text{TCNE}]^- \cdot x(1,3\text{-C}_6\text{H}_4\text{Cl}_2)$  at differing applied fields for (a)  $T=5.0$  K and (b)  $T=2.5$  K. The symbols represent the data and the dashed lines correspond to the best fit to Eq. (2).

respectively), while the value of  $\sigma_0$  is 717 and 5038 Oe, respectively. For the data below  $T_g$  at 2.5 K [Fig. 5(b)], the value for  $\tau$  is very long ( $\tau \sim 10^5$  s) as expected for temperatures below the spin glass freezing transition. A good fit to Eq. (2) was not possible for the data taken at 22.5 kOe which lies near the coercive field value at this temperature.

#### D. ac measurements

To probe the response of the system on shorter time scales, measurements of the ac susceptibility were recorded from 4.5 to 50 K, at frequencies from 11.0 Hz to 11.0 kHz with an ac field of 1.0 Oe and zero applied dc field (Fig. 6). The data for 11.0 Hz was fit to a theoretical prediction for the dynamics of a 1D infinite Ising spin chain<sup>18</sup>

$$\chi' = \frac{\mu^2 N (1 + \eta)}{kT} \frac{\alpha^2 (1 - \gamma)^2}{1 - \eta \alpha^2 (1 - \gamma)^2 + \omega^2} \quad (3)$$

with  $\gamma = \tanh(2J/kT)$ ,  $\eta = \tanh(J/kT)$ , and  $\alpha = 1/\tau$ . Fits were made assuming Arrhenius behavior with an activation energy equal to  $J/k$ .

The best fit to Eq. (3) (Fig. 6) was obtained for a value of  $J/k = 14.8$  K, well below the experimentally determined

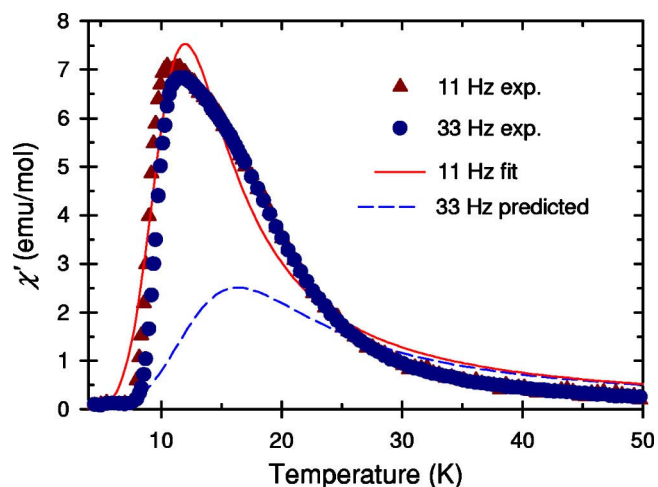


FIG. 6. (Color online) Fits of  $\chi'$  data to a model of an infinite 1D Ising spin chain. The fit to the 11 Hz data is unable to account for the observed broad, asymmetric peak. Further, the predicted curve for a frequency of 33 Hz [as obtained by assuming the constants of Eq. (3) are frequency independent] lies much below the actual experimental data.

value of over 100 K (Refs. 1 and 9) found for the intrachain exchange. Further, the fit is unsatisfactory in explaining the rich structure of the experimentally measured peak. In particular, the theoretical predictions cannot explain the presence of the broad asymmetric peak. In addition, by assuming frequency independent fitting parameters ( $J$ , etc.), theoretical predictions of  $\chi'$  for 33 Hz were calculated. The results show a peak which is greatly reduced from the calculated fit of the 11 Hz data. This reduction is much greater than the experimentally observed decrease between the 11 and 33 Hz  $\chi'$  data.

#### IV. DISCUSSION

The relaxation of the system at various applied fields (Fig. 5) provides key data to understanding the reversal mechanism in  $[\text{MnTPP}]^+[\text{TCNE}]^- \cdot x(1,3\text{-C}_6\text{H}_4\text{Cl}_2)$ . This data shows the time-dependent behavior at key points along the hysteresis loop. We see that for temperature above  $T_g$  appreciable change occurs to the magnetization for time scales  $< 10^3$  s. While for  $T < T_g$ , the value of the magnetization is essentially constant over this time range for values of the applied field less than  $H_c$ . As  $H_c$  is approached, the data can no longer be fit with a stretched exponential, implying a different relaxation mechanism occurs for this region.

For most systems, this type of in-field relaxation occurs too rapidly or over too small of a temperature range to study its effects on typical magnetic measurements. In this system, the unique fractal nature of the spin clusters causes a slow, viscous relaxation process. This extremely slow relaxation leads to the observed dramatic shifts in the hysteresis loops shown in Fig. 2 as well as in the ZFC magnetization curves of Fig. 1.<sup>13</sup>

The FC/ZFC magnetization curves show typical spin glass behavior. The small, constant value of the ZFC magne-

tization at low temperatures even at high fields (up to 1000 Oe) suggest a frozen spin glass state. The spins are strongly held in the low spin state until the temperature is increased above  $T_g$ . Near this point a sharp increase in magnetization to the FC value occurs, in accord with the viscous behavior and long relaxation times observed in this system.

The effect of the long relaxation times is evident in Fig. 1 where the ZFC magnetization shows a shift in the bifurcation point to lower temperatures with longer waiting times. These long relaxation times above the glass transition keep the system in a nonequilibrium state for measurements on normal laboratory time scales (time between measurements less than one hour). For experiments in the equilibrium state, the bifurcation should occur at the glass transition. In this system the slow relaxation prevents equilibrium state measurements at normal laboratory time scales and is responsible for the observed bifurcation temperatures being well above the glass transition temperature of  $\sim 4$  K.

The time-dependent effects seen in the hysteresis curves above the glass transition (Fig. 2) are evidence of magnetic relaxation at high temperatures. When the response times of the system are on the order of the time scale of measurements, it is possible to record hysteresis curves at different stages of the spin relaxation by adjusting the time between measurements. Our data show a larger coercive field when the applied field is ramped at a higher rate, in agreement with theoretical calculations on spin glasses.<sup>19</sup> The observation of this type of relaxation at temperatures well above the glass transition temperature is unusual for traditional 3D spin glasses. However, due to the unique quasi-1D nature of this system, the transition region covers a large range of both temperatures and relaxation times.<sup>13</sup> To our knowledge, the 170% change in  $H_c$  of Fig. 2 represents the largest such increase reported.

The shapes of the minor hysteresis loops of Fig. 3 also show evidence of magnetic relaxation. The loops are rounded at the edges as the system has not fully relaxed to the desired magnetization prior to reduction of the applied field strength. This relaxation is also responsible for the loop remaining open upon completion of the cycle. Further, a magnetic history effect is clearly evident by the stark differences between the forward and reverse loop.

We propose that these relaxation effects above  $T_g$  reflect the fractal spin glass state formed at lower temperatures. Magnetic relaxation has been reported in other chain compounds.<sup>1,21-23</sup> For some of these systems<sup>21-23</sup> the relaxation has been proposed to occur according to the 1D infinite chain Ising model of Glauber.<sup>18</sup> However, fits of the susceptibility of  $[\text{MnTPP}]^+[\text{TCNE}]^- \cdot x(1,3\text{-C}_6\text{H}_4\text{Cl}_2)$  to this purely 1D model (Fig. 6) were unsatisfactory. Also, the presence of a distribution of relaxation times in this system, as observed by Cole-Cole analysis of the ac susceptibility<sup>11</sup> and the stretched exponential decay of the thermoremanent magnetization,<sup>13</sup> is consistent with spin glass behavior and not isolated 1D chains. We note that a fractal spin ground state may occur in other nearly 1D magnetic chain systems.

An anisotropic fractal cluster model explains the long relaxation times observed in this system. Frustration in this system has been attributed to competition between the single-ion anisotropy of manganese and the interchain dipole-

lar interactions.<sup>1</sup> As the dipole-dipole interactions are long range, the frustration can be over many chains and prohibit the system from reaching an equilibrium state. In this way the dipolar interactions between the anisotropic clusters can lead to a shift of characteristic response times toward longer time scales, similar to effects caused by dipolar interactions in ferrofluids.<sup>6,7</sup>

The  $H_c(T)$ , Fig. 4, provides insight into the mechanism for magnetic reversal. At low temperatures  $H_c$  is nearly linear in  $T$ , suggesting a temperature independent energy barrier responsible for magnetic reversal leading to  $H_c(T \rightarrow 0) \approx 40$  kOe. A linear temperature dependence for  $H_c$  has been predicted for domain wall systems for the case of weak pinning.<sup>17</sup> In the case of a spin glass, this corresponds to strongly interacting spin clusters where many clusters reverse their magnetization simultaneously. Cooperative behavior also is suggested by the squareness of the hysteresis loops below  $T_g$  when compared with the higher temperature loops (Fig. 2). For higher temperatures,  $H_c(T)$  is no longer linear, but takes the form of Eq. (1). This form has been predicted<sup>17</sup> for a system with strongly pinned domain walls; for a cluster model this corresponds to weakly interacting spin clusters.

The presence of the crossover from weakly to strongly interacting clusters is predicted from the fractal nature of the spin clusters in the system.<sup>13</sup> Below  $\sim 5$  K, the system begins to have spin clusters of dimension slightly greater than one. This implies that below this temperature, the clusters branch out into multiple chains within the material. The lack of interchain exchange pathways leads to anisotropic clusters which are largely confined to a single chain, while branching out to neighboring chains at various locations. This branching then enhances the interaction between clusters, stabilizing neighboring clusters into cooperative units and forcing the system into the frozen spin glass state. This stabilization of neighboring spin clusters is one factor leading to the large observed coercive fields in this material. It has not escaped our attention that a similar enhancement of interaction strength could occur in other interpenetrating systems, for example, interacting polymer chains in solution<sup>24</sup> and fractal aggregation on magnetic multilayers.<sup>25</sup>

## V. CONCLUSIONS

In sum, the role of the fractal spin clusters in magnetic relaxation has been investigated in the organic-based magnet  $[\text{MnTPP}]^+[\text{TCNE}]^- \cdot x(1,3\text{-C}_6\text{H}_4\text{Cl}_2)$ . Frustration induced by the long-range dipole-dipole interactions between fractal spin clusters hinders magnetic reversal and causes extremely long magnetic relaxation times as observed in the in-field magnetic relaxation data (Fig. 5). This slow stretched exponential relaxation has a dramatic effect on typical magnetic measurements. Above  $T_g$ , in the region where the fractal spin clusters behave independently, dynamic hysteresis measurements show the value of  $H_c$  to be strongly dependent on the sweep rate of the applied magnetic field. To our knowledge, rate-dependent hysteresis has not been reported in traditional 3D spin glasses at temperatures approaching  $T/T_g = 1.3$  as presented here for this fractal cluster system. Below  $T_g$ , both

the shape of the hysteresis loops and the linear temperature dependence of  $H_c$  indicate collective behavior of spin clusters in an anisotropic fractal cluster picture. In this lower-temperature region, the branching of spin clusters into neighboring chains forces the more collective behavior, with the intermingling of clusters leading to an enhanced coercivity at low temperatures. Attempts to model the magnetic relaxation

to a simple 1D model were unsuccessful furthering support for the fractal interpretation.

#### ACKNOWLEDGMENTS

This work was supported in part by the DOE, Grant No. DE-FG02-86ER45271 and the NSF, Grant No. CHE-0110685.

- 
- <sup>1</sup>C. M. Wynn, M. A. Girtu, W. B. Brinckerhoff, K. I. Sugiura, J. S. Miller, and A. J. Epstein, *Chem. Mater.* **9**, 2156 (1997).
- <sup>2</sup>S. Ostrovsky, W. Haase, M. Drillon, and P. Panissod, *Phys. Rev. B* **64**, 134418 (2001).
- <sup>3</sup>A. Caneschi, D. Gatteschi, J. P. Renard, P. Rey, and R. Sessoli, *Inorg. Chem.* **28**, 1976 (1989).
- <sup>4</sup>B. C. den Hertog and M. J. P. Gingras, *Phys. Rev. Lett.* **84**, 3430 (2000).
- <sup>5</sup>R. G. Melko, B. C. den Hertog, and M. J.P. Gingras, *Phys. Rev. Lett.* **87**, 067203 (2001).
- <sup>6</sup>C. Djurberg, P. Svedlindh, P. Nordblad, M. F. Hansen, F. Bødker, and S. Mørup, *Phys. Rev. Lett.* **79**, 5154 (1997).
- <sup>7</sup>T. Jonsson, P. Nordblad, and P. Svedlindh, *Phys. Rev. B* **57**, 497 (1998).
- <sup>8</sup>J. García-Otero, M. Porto, J. Rivas, and A. Bunde, *Phys. Rev. Lett.* **84**, 167 (2000).
- <sup>9</sup>W. Hibbs, D. K. Rittenberg, K. I. Sugiura, B. M. Burkhart, B. G. Morin, A. M. Arif, L. Liable-Sands, A. L. Rheingold, M. Sundaralingam, A. J. Epstein, and J. S. Miller, *Inorg. Chem.* **40**, 1915 (2001).
- <sup>10</sup>C. M. Wynn, M. A. Girtu, K. I. Sugiura, E. J. Brandon, J. L. Manson, J. S. Miller, and A. J. Epstein, *Synth. Met.* **85**, 1695 (1997).
- <sup>11</sup>M. A. Girtu, C. M. Wynn, K. I. Sugiura, J. S. Miller, and A. J. Epstein, *J. Appl. Phys.* **81**, 4410 (1997).
- <sup>12</sup>J. Seiden, *J. Phys. (Paris), Lett.* **44**, L947 (1983).
- <sup>13</sup>S. J. Etzkorn, W. Hibbs, J. S. Miller, and A. J. Epstein, *Phys. Rev. Lett.* **89**, 207201 (2002).
- <sup>14</sup>K. Nagai, T. Iyoda, A. Fujishima, and K. Hashimoto, *Chem. Lett.* **1996**, 591 (1996).
- <sup>15</sup>D. K. Rittenberg, K. I. Sugiura, Y. Sakata, S. Mikami, A. J. Epstein, and J. S. Miller, *Adv. Mater. (Weinheim, Ger.)* **12**, 126 (2000).
- <sup>16</sup>K. Nagai, L. Jiang, T. Iyoda, A. Fujishima, and K. Hashimoto, *Thin Solid Films* **331**, 165 (1998).
- <sup>17</sup>P. Gaunt, *Philos. Mag. B* **48**, 261 (1983).
- <sup>18</sup>R. J. Glauber, *J. Math. Phys.* **4**, 294 (1963).
- <sup>19</sup>P. N. Timonin, *Phys. Rev. B* **52**, 7295 (1995).
- <sup>20</sup>It should also be noted that  $H_c$  values may vary by up to 10% depending on the conditions during sample synthesis. All data in Fig. 4 were taken on sample from the same batch, while data in other figures were taken on samples from another batch.
- <sup>21</sup>A. Caneschi, D. Gatteschi, N. Lalioti, C. Sangregorio, R. Sessoli, G. Venturi, A. Vindigni, A. Rettori, M. G. Pini, and M. A. Novak, *Angew. Chem., Int. Ed.* **40**, 1760 (2001).
- <sup>22</sup>A. Caneschi, D. Gatteschi, N. Lalioti, C. Sangregorio, R. Sessoli, G. Venturi, A. Vindigni, A. Rettori, M. G. Pini, and M. A. Novak, *Europhys. Lett.* **58**, 771 (2002).
- <sup>23</sup>R. Clérac, H. Miyasaka, M. Yamashita, and C. Coulon, *J. Am. Chem. Soc.* **124**, 12837 (2002).
- <sup>24</sup>S. Kumar and Y. Singh, *Phys. Rev. E* **51**, 579 (1995).
- <sup>25</sup>F. Yang and F. Pan, *Phys. Rev. E* **64**, 051402 (2001).